Supplementary Information for
Observation of metastability in open quantum dynamics of a solid-state system

Jun-Xiang Zhang,[1,2,*] Yuan-De Jin,[3,4,*] Chu-Dan Qiu,[3,4] Wen-Long Ma,[3,4,†] and Gang-Qin Liu[1,2,5,‡]

[1] *Beijing National Laboratory for Condensed Matter Physics and Institute of Physics, Chinese Academy of Sciences, Beijing 100190, China*
[2] *School of Physical Sciences, University of Chinese Academy of Sciences, Beijing 100049, China*
[3] *State Key Laboratory of Superlattices and Microstructures, Institute of Semiconductors, Chinese Academy of Sciences, Beijing, 100083, China*
[4] *Center of Materials Science and Opto-Electronic Technology, University of Chinese Academy of Sciences, Beijing 100049, China*
[5] *CAS Center of Excellence in Topological Quantum Computation, Beijing 100190, China*

[*] These authors contributed equally to this work

[†] wenlongma@semi.ac.cn

[‡] gqliu@iphy.ac.cn

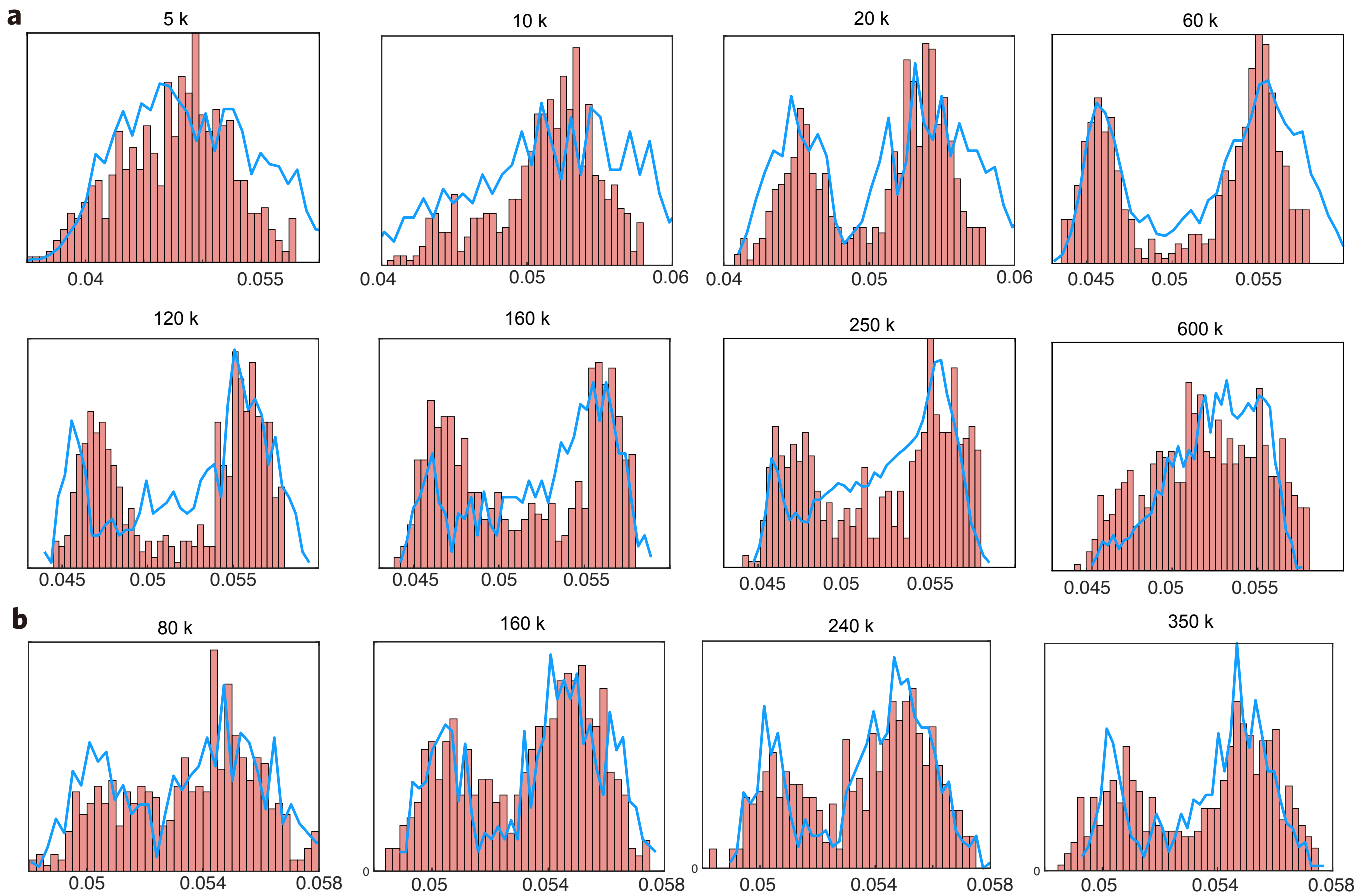

Figure S1. **a**, Statistical results of the PL trace of the experiment with magnetic field tilt angle $7^{\circ} \pm 2^{\circ}$ and $\tau = 374$ ns (data of 5 k, 60 k, 250 k, 600 k are shown in Fig. 2**c**). **b**, Another experiment with the magnetic field tilt angle of $8^{\circ} \pm 2^{\circ}$ and $\tau = 370$ ns, The simulation in **b** is performed under $\theta = 7.94^{\circ}$, which is close to the value measured in the experiment.

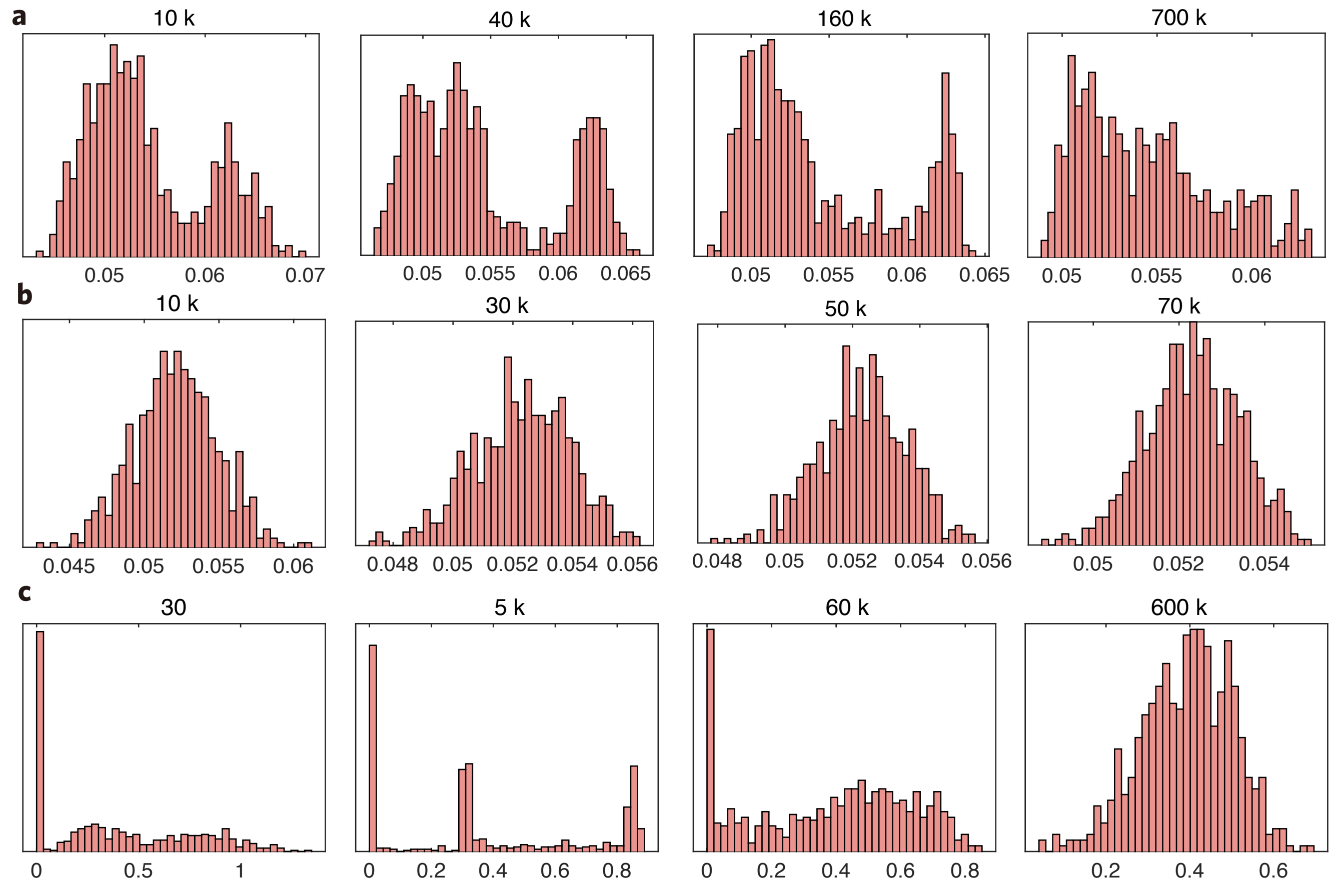

Figure S2. **Histogram of the results of the Monte Carlo simulation.** The parameters of **a** and **b** are **a** $\theta = 3.5^{\circ}$ and **b** $\theta = 15^{\circ}$ with weak measurement ($n_0 = 0.065$ and $n_1 = 0.049$). **c**, Numerical simulation results with strong measurement ($n_0 = 0$ and $n_1 = 1$) with $\theta = 8.8^{\circ}$.

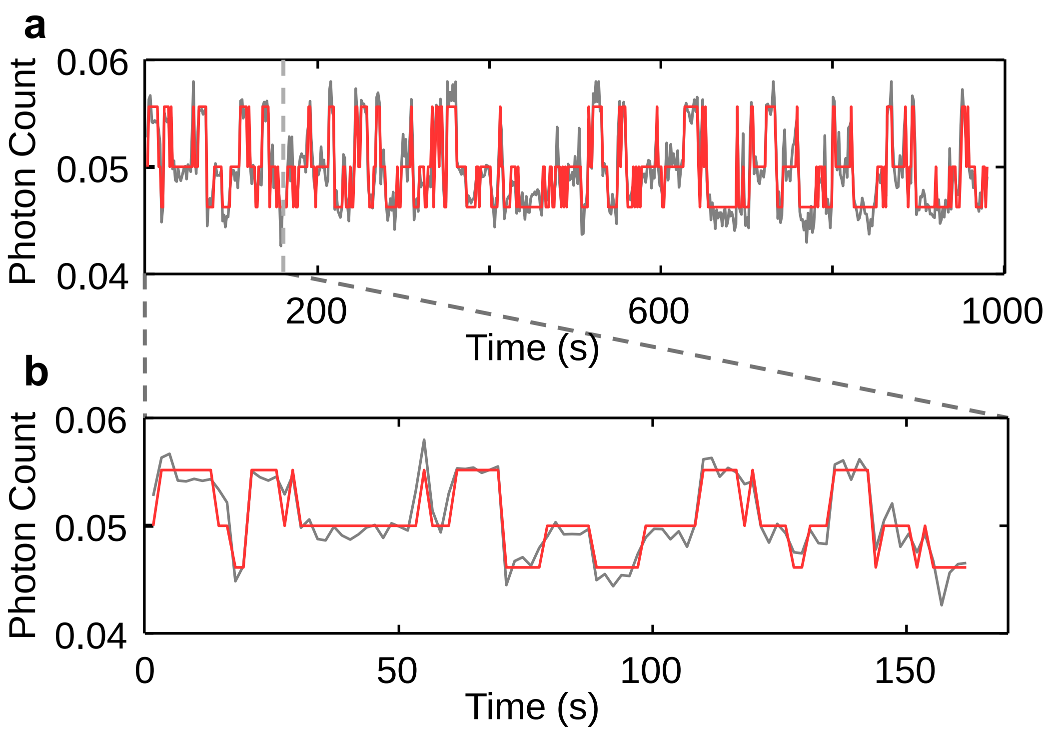

Figure S3. **Triple-peak quantum jumps.** **a**, With a slight misalignment of the magnetic field with respect to the NV axis, the signal of triple-peak quantum jumps is observed at the RIM duration $\tau = 350$ ns, $m = 60$ k. The red fitting line is extracted from the HMM model. **b**, The first 100 points of of triple-peak quantum jumps signal.

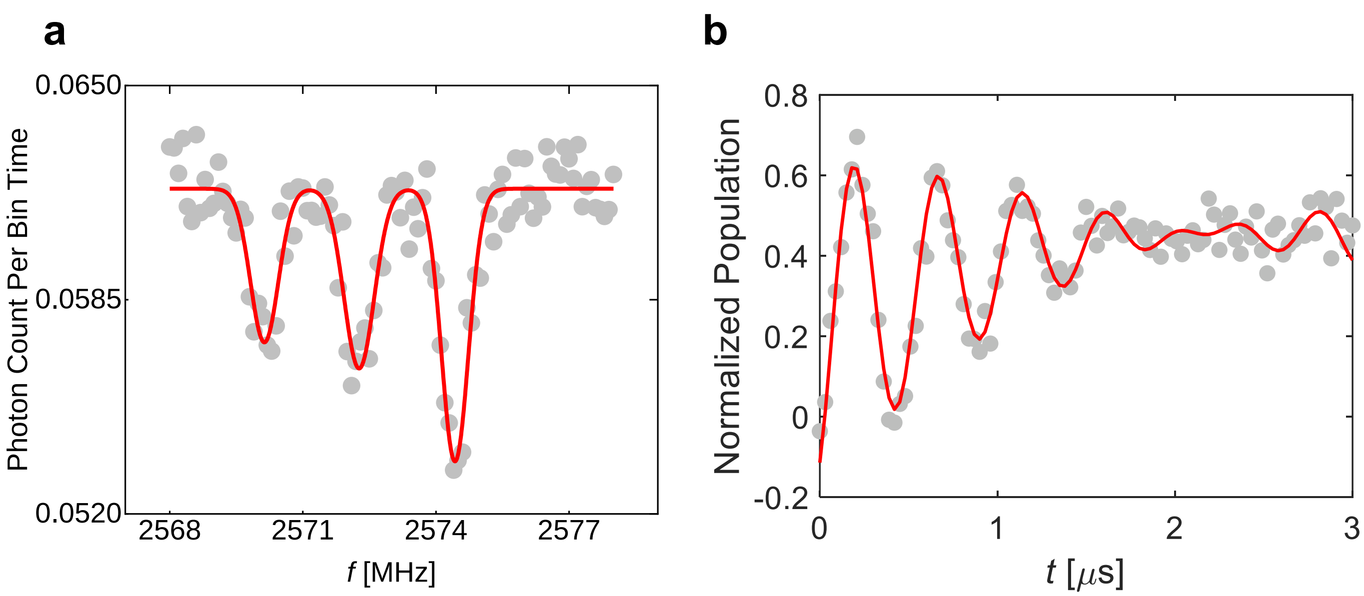

Figure S4. **Pulse-ODMR and FID signal of the NV center.** **a**, Pulsed-ODMR spectrum of the NV electron spin. The resonances correspond to the ^{14}N nuclear spin sublevels under an external magnetic field of $B_z \approx 108.4$ G. The data are fitted by a 3-peak Gaussian function. **b**, Ramsey signal of the NV spin giving the $T_{2e}^{*} = 2.9$ μs.

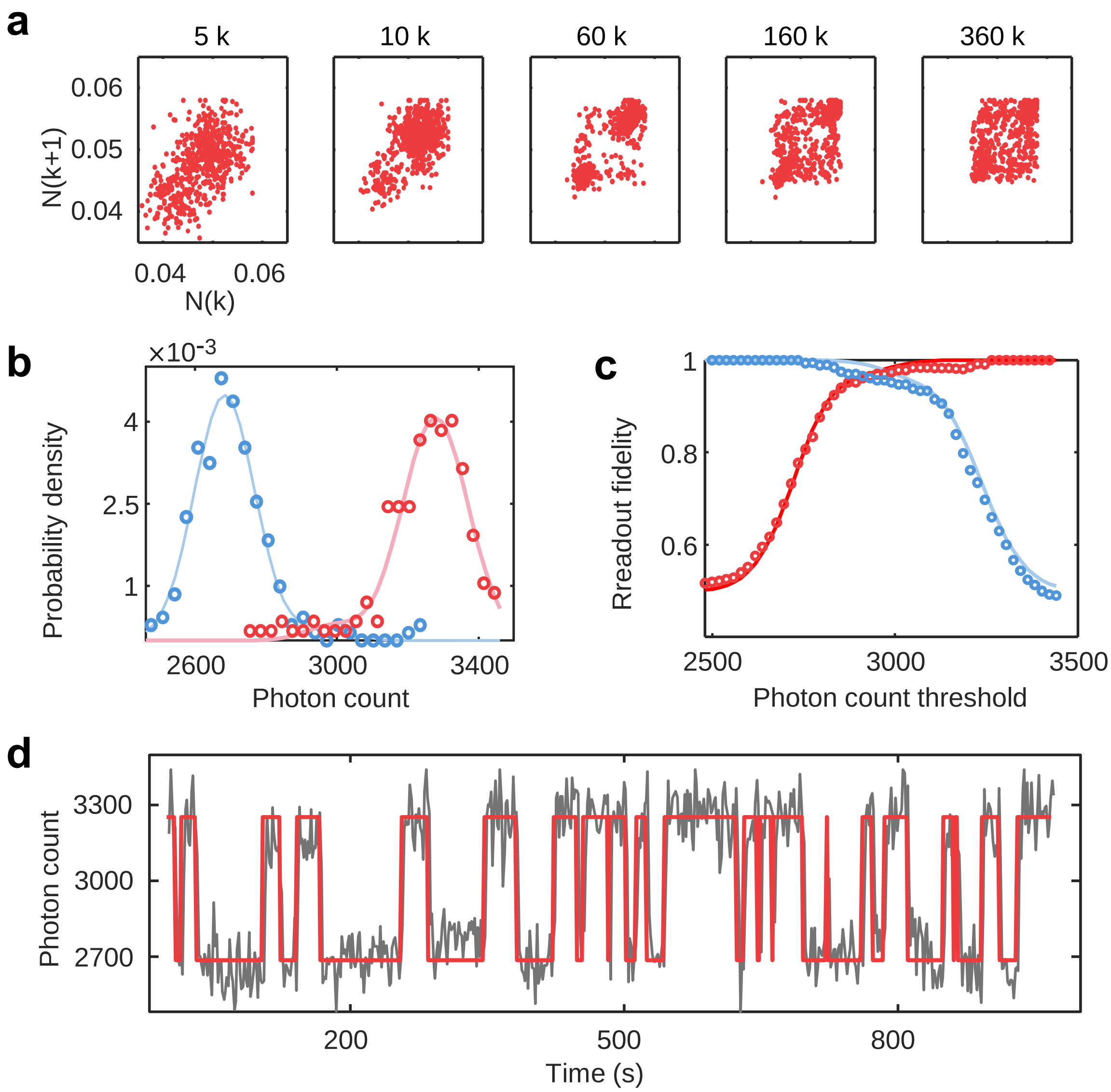

Figure S5. ^{14}**N nuclear spin readout fidelity.** **a**, The distribution of two consecutive measurements, $N(k)$ and $N(k+1)$, from the PL time trace recorded by continuous application of the single-shot readout sequence. A clear transition from the thermal state to the metastable state, and then to the thermal state is observed. **b**, The histograms of photon counting depending on the nuclear spin state, the measurement number m = 80 k. **c**, Fidelity of the single-shot readout of the ^{14}N nuclear spin as a function of the readout threshold. **d**, PL time trace with quantum jumps of the ^{14}N nuclear spin state. The red-filled data are fitted by a three-state hidden Markov model from which the relaxation time T_1 of the nuclear spin state can be extracted.

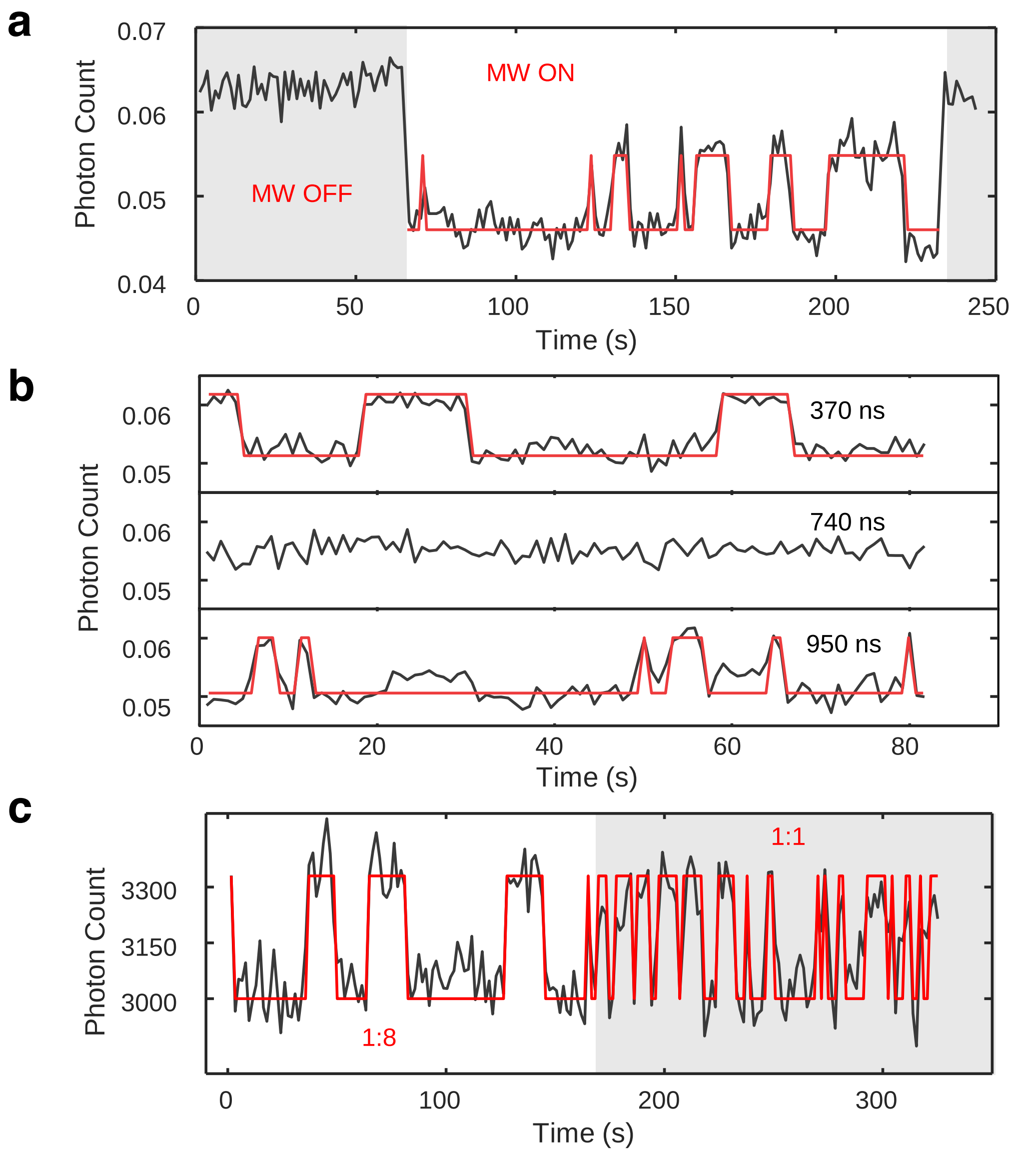

Figure S6. **PL time trace under different experimental conditions** **a**, By switching the microwave pulse on and off, the quantum jump signals can be switched on and off accordingly. **b**, The PL time trace for RIM duration of $\tau = 370$ ns, 740 ns, and 950 ns under a certain magnetic field orientation. **c**, For a fixed total length of the RIM sequence, setting the optical excitation duty cycle and wait time from $1:8$ to $1:1$ (as highlighted by the gray shadow region) allows a direct acceleration of the jump rate. These results suggest that the spin relaxation (T_{1n}) of the ^{14}N nuclear spin is dominated by flips induced by hyperfine interactions in the excited NV state, which can be triggered by the optical excitation process.